Grant Agreement No. 611373

FP7-ICT-2013-10

D1.3. Report on integration of the robotic assistant system - experiments and performance

Due date of deliverable: 30/05/2015
Actual submission date: 28/07/2015

Start date of project: 01 January 2014 Duration: 36 months

Organization name of lead contractor for this deliverable: CNR

Version 1

Dissemination level		
PU	Public	x
PP	Restricted to other programme participants (including the Commission Services)	
RE	Restricted to a group specified by the consortium (including the Commission Services)	
CO	Confidential, only for members of the consortium (including the Commission Services)	

Contents

1 Outline of the deliverable

This deliverable provides a description of the initial experiments and performance analysis of the CADDY systems capabilities. The report describes the final hardware integration of the primary and backup vehicles, as well as the software modules developed to achieve the required functionalities. Simulation results were performed to evaluate the reliability of the different software components needed to fulfill the different CADDY sub-goals, while experimental trials provided data for performance analysis of the system.

2 Hardware integration

This section reports the description of the final hardware integration operations performed on the different primary and backup robotic platforms involved in the CADDY framework.

2.1 Primary robotic platforms

2.1.1 MEDUSA$_S$

The autonomous surface vehicles of the MEDUSA-class (henceforth referred to as MEDUSA$_S$), are approximately 1035 mm long and weigh 23-30 kg (depending on their configuration). Their housings consist of two 150 mm diameter acrylic tubes with aluminum end caps, attached to a central aluminum frame, see the figure below. This design allows for a better weight distribution in terms of metacentric height, and shorter length. As a result, the vehicles are easy to transport and launch and have good static stability. The upper body carries the light components, namely a single-board computer, an RTK-enabled GPS receiver, Wi-Fi 802.11 communications, a full navigation sensor suite, and a video acquisition system for an underwater camera. Most of the weight is concentrated in the lower body where the LiPo (Lithium Polymer) batteries and power management electronics are installed. Each of the MEDUSA$_S$ vehicles is propelled by two side-mounted, forward-facing thrusters that yield surge and yaw motion: the vehicle is capable of reaching speeds up to 1.5 m/s with respect to the water. As will be explained later, the diving version of the MEDUSA class of vehicles (referred to as MEDUSA$_D$) are also equipped with two vertical thrusters for controlled motion in the vertical plane.

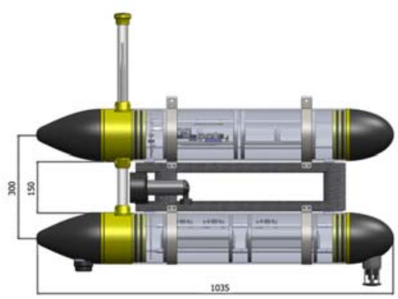

MEDUSA$_S$ (Surface) Particulars	
Length	1035 mm
Height	875 mm
Tube diameter	150 mm
Weight in air	23 kg (Surface), 30 kg (Diver)
Energy	830 Wh LiPo
Endurance	11 h at 1.5 knots
Propulsion System	2 thrusters (Surface) 4 thrusters (Diver)

Fig. 3.1.1 The MEDUSA class of vehicles (MEDUSA$_S$): main particulars

As part of the effort to afford the members of the CADDY project marine vehicles to test and assess the efficacy of the methods developed for cooperative motion control, the MEDUSA vehicles of IST were upgraded and fully tested, as explained below. *All existing MEDUSA vehicles can be used as ASVs (Autonomous Surface Vehicles)*. In this mode of operation, they are simply referred to as MEDUSA$_S$ vehicles (where S stands for "Surface"). *Two of them have been upgraded in terms of sensors, actuators, power distribution, and control systems to be able to dive and can therefore be used as AUVs (Autonomous Underwater Vehicles)*. In this mode of operation, they are referred to as MEDUSA$_D$ vehicles (D stands for "Diver"). This was done in view of the goals to : i) develop and assess, under real operational conditions, the performance obtained with cooperative navigation and control systems for surface and underwater vehicles carrying joint missions (e.g., performing a leader tracking maneuver whereby the CADDY ASV plays the role of leader and the CADDY AUV tracks the trajectory described by the leader), and ii) to evaluate the performance of the navigation and control systems developed to allow for close diver / CADDY AUV interaction. In fact, it is envisioned that from a pure motion control and navigation standpoint, one of the underwater vehicles will act as a proxy for the diver during the first part of the project. Because of the role (as testbeds) that the MEDUSA vehicles will play in the CADDY project, the *work done aimed also at adapting the software architecture of both the* $MEDUSA_S$ *and* $MEDUSA_D$ *vehicles according to the rules defined by the partner group for heterogeneous systems integration*.

To reduce the exposure to human divers, a new carbon fiber frame was installed on the MEDUSA vehicles in order to hide any sharp edges. Thruster blades are also well covered with a protective nozzle.


Fig. 3.1.2 a) A $MEDUSA_S$ *vehicle with the new carbon fiber frame b) thrusters protective nozzle*

For navigation and control purposes, the Seatrac USBL unit was installed in the lower body of one the MEDUSA vehicles. Preliminary trials aiming at assessing the performance of the unit were conducted at the EXPO 98 site, Lisbon, Portugal; they will be described later in this document.

Fig. 3.1.3 Seatrac USBL mounted on Medusa Yellow

2.1.2 Buddy

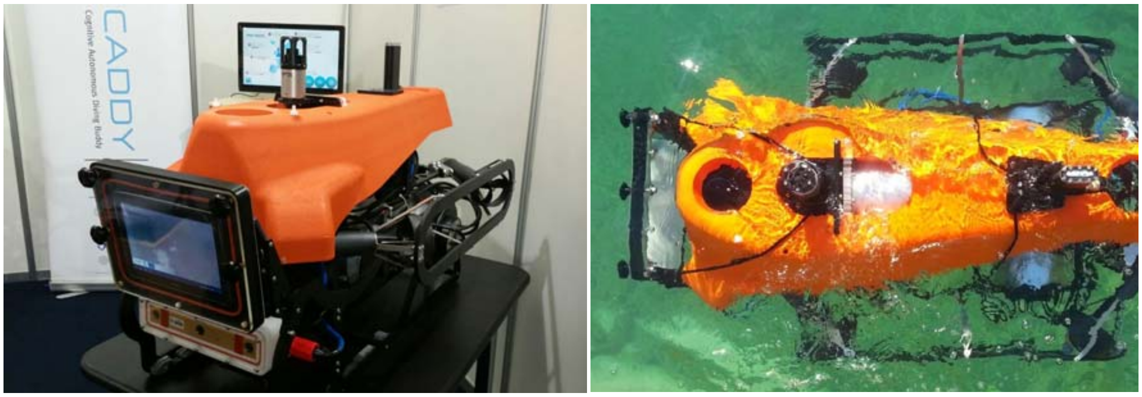

Fig. 3.1.1. The Buddy vehicle during assembly and in water

Hardware and software integrations on the Buddy vehicle includes:

1. Low-level sensor network
2. USBL and ARIS multi-beam sonar integration
3. Thruster mapping and allocation
4. Floating-block integration
5. Vehicle control and navigation

Fully integrated low-level sensors are pressure, temperature, and leak detectors across cylinders. The low-level analog sensors are sampled across Buddy cylinders by Arduino Micro microcontrollers that are connected in a low-level communication network in order to distribute the measurement to the two main computers, the vision and master cylinder computer. The approach allows for easy addition of new low-level sensors, if necessary, to ensure proper vehicle functioning. Two of the three microcontrollers are exposed to the ROS systems running on the embedded computers as single nodes that accept and exchange information with the ROS eco-system. This is achieved by use of the ROS-serial communication protocol developed by the ROS community for microcontroller integration in larger ROS systems.

The Seatrac USBL sensor was mounted on the vehicle and connected to the master cylinder. The communication and ranging was tested in Biograd 2015 integration trials. Further the ARIS sonar and stereo camera were integrated on the Buddy vehicle and their functionality was validated on the same integration trials.

Thruster mapping was performed on the mounted Pro4 thrusters and their characteristic was identified to improve the integration of control algorithms. The nonlinear characteristic of each thruster when mounted on the vehicle is shown in Figure 3.1.1. Quadratic model fitting was applied to the thruster to utilize existing thruster models from ROS. However, in future a better fit can be achieved by using a polynomial fit with more degrees of freedom since the thrusters exhibit a more complex nonlinearity than the usual quadratic dependency between voltage and achieved force. Observe that the fore thrusters are weak in the reverse direction although they still require the same current as aft thrusters which achieve a noticeably higher thrust force. This is attributed to the fact that the flow of the fore thrusters in reverse direction is hindered by the underwater tablet mounted on the vehicle. The tablet position is a result of requirements that the tablet has to be mounted safely (away from thrusters) and be easily accessible. Although the design cannot be changed without breaking the tablet mounting requirements the thruster allocation can take into account the weaker behavior of fore thrusters. To reduce energy consumption the fore thrusters will be considered high-cost in reverse direction during allocation. The fore vertical thruster also exhibits a weakened behaviour due to lack of proper water flow behind the underwater tablet.

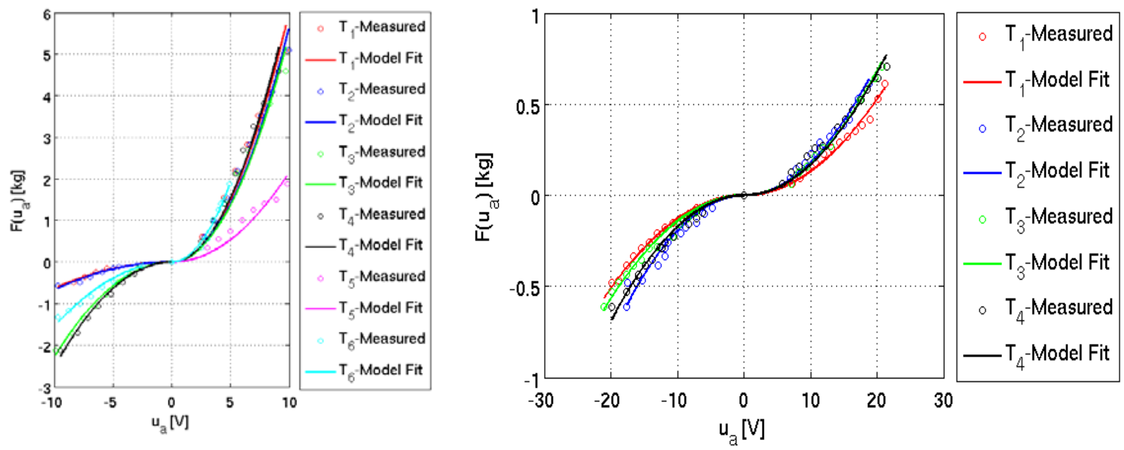

(a) *(b)*

Fig. 3.1.2. Mapped and fitted thrust model (F=Kua|ua|); (a) Buddy thrusters and (b) PlaDyPos thrusters

The hardware integration included the mounting and testing of the floating block, see Figure 3.1.1, which was missing during previous test. The vehicle was trimmed and the complete model identification with navigation, guidance and control was performed on the completed vehicle.

During the integration trials the Buddy model identification for horizontal degree of freedom was performed. The time and location constraints inhibited identification of the heave degree of freedom. The identified parameters are shown in Table 3.1.1. Low-level velocity controllers were adjusted and the EKF estimator was tuned to filter very noisy DVL measurements with the identified surge and sway models. High-level controllers for heading and dynamic position were tuned and implemented. Figure 3.1.3 show the Buddy responses to heading and surge commands.

Problems with the thruster controller operation were encountered during the integration trials. The thrusters are brushless VideoRay Pro4 thrusters running on a commercial off-the-shelf M5 controller. The controllers stopped working after prolonged periods of usage and required hardware resetting via the control relays. In order to alleviate this problem the PlaDyPos custom made drivers, shown to work robustly, are considered as replacement driver for the Buddy vehicle.

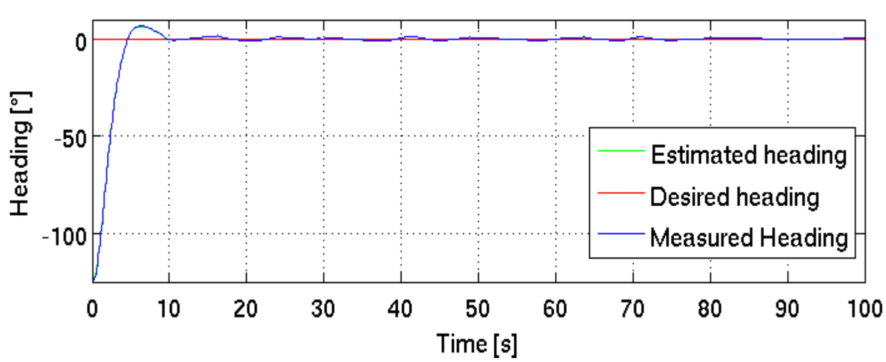

(a)

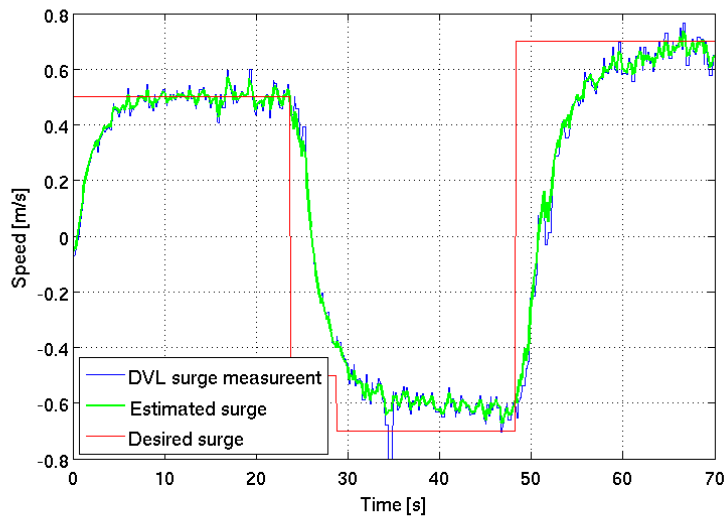

(b)

Fig. 3.1.3. (a) Heading response and (b) surge speed response of the Buddy vehicle

DoF	α [norm]	β_{υ} [norm]	$\beta_{\|\upsilon\|\upsilon}$ [norm]	ω_n [rad/s]
surge	4.471	0.860	2.044	0.377
sway	8.523	2.001	8.317	0.266
yaw	1.321	0.302	0.446	0.843

Table 3.1.1. The horizontal identified DoF for the Buddy vehicle

2.2 Backup robotic platforms

2.2.1 PlaDyPos

Fig. 3.2.1. PlaDyPos vehicle on shore and in water

The PlaDyPos vehicle, Figure 3.2.1, was refurbished to allow easier battery exchange and new sensor integrations. A down-looking camera mounting, Seatrac USBL and ARIS sonar exchangeable mount were developed. The down-looking camera, Bosch Starlight VR7000, can be used to visually validate the position of the diver or a ROV used to simulate the diver during initial tests, see Figure 3.2.2. The factory USBL cage was removed and a new wider cage constructed to protect the hydrophone heads and reduce the cage influence on the USBL precision.

(a) (b)

Fig. 3.2.2. (a) PlaDyPos camera for tracking validation in shallow water and (b) custom made USBL cage

The lithium-ion batteries were replaced with AGM batteries to allow easier airline transport and reduce the platform cost. The advantage is that PlaDyPos plug'n'play exchangeable, fast charging batteries for longer autonomy. The disadvantage is that the vehicle is heavier and requires a two-person deployment. The vehicle was additionally outfitted with Novatel GPS supporting dGPS corrections in order to improve the positioning accuracy. A dGPS station was constructed with a second Novatel GPS to offer easy and transportable relative navigation near the shore-side. One additional benefit is that the AGM batteries are connected to offer easy switching from 24 V to 12 V operations which will allow testing of potential new thrusters arriving on the market.
Due to refurbishment the vehicle had to undergo a similar mapping procedure to the Buddy vehicle. The thruster mapping can be seen in Figure 3.1.2b. Similarly model identification was performed and the parameters are shown in Table 3.2.1.

DoF	α [norm]	β_{υ} [norm]	$\beta_{\|\upsilon\|\upsilon}$ [norm]	ω_n [rad/s]
surge	4.152	1.837	4.709	0.277
yaw	0.445	0.229	0.229	1.472

Table 3.2.1. The identified DoF for the PlaDyPos vehicle (Note: the vehicle is symmetric in surge and sway)

The EKF navigation and low-level controllers were re-adjusted with the new parameters and the high-level controllers were tested. The station-keeping and acoustic localization algorithms were tested and validated. High level primitives that will be necessary for future trials were tested. Additionally, primitives, navigation filters and estimators that will be useful with the Buddy vehicle were tested on PlaDyPos to validate algorithms while the Buddy vehicle was assembled.

Range-only target tracking primitive with extremum-seeking localization was tested on PlaDyPos and is shown in Figure 3.2.3. Further, Figure 3.2.4 shows a lawn-mower mission executed with GoTo primitives.

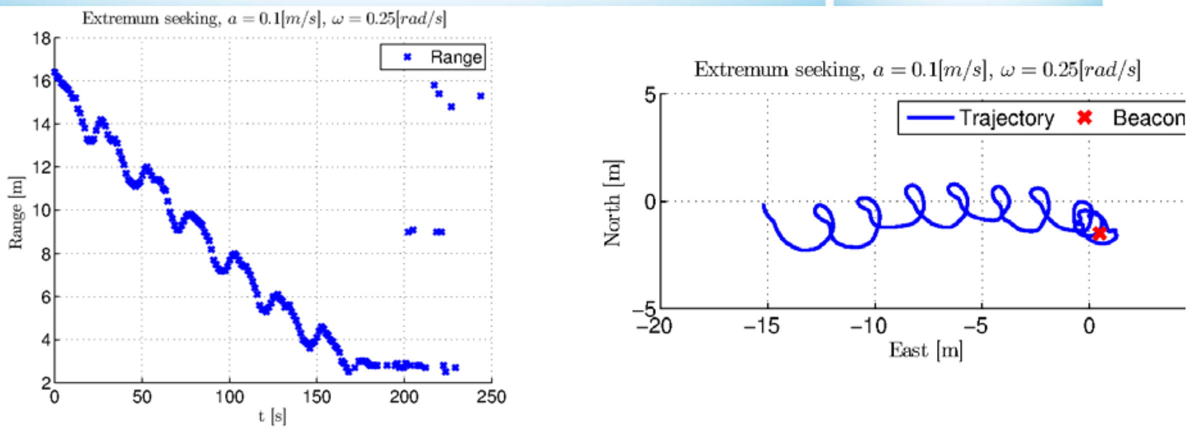

(a) *(b)*

Fig. 3.2.3. PlaDyPos extremum-seeking tracking of the object with range-only measurements

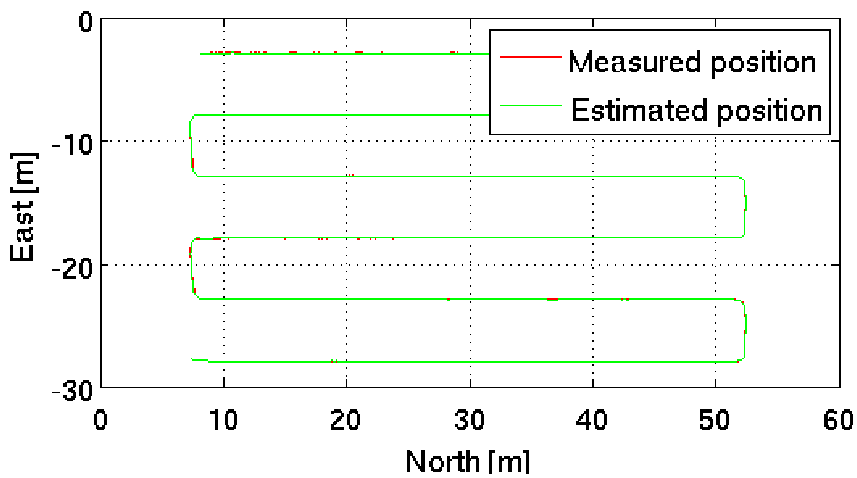

Fig. 3.2.3. PlaDyPos lawn-mower mission with GoTo primitives

2.2.2 MEDUSA$_D$

For the CADDY project, the “BUDDY” vehicle needs to maintain itself in the field of view of the human diver (to allow the diver to see it) while simultaneously i) keeping the human diver in its own field of view (for camera/ sonar based diver tracking) and ii) following arbitrary paths or illuminating the seafloor in arbitrary directions. To be able to perform these manoeuvres the “BUDDY” vehicle is required to have lateral actuation. As such, with the objective of contributing to the pool of vehicles available for tests in the scope of the project, the MEDUSA$_D$ vehicles are being modified to accommodate a new additional thruster with custom mechanical parts developed in-house. Moreover, the leader tracking and underwater path-following controllers are being redesigned to take advantage of the vehicle sway motion.

Fig. 3.2.1 and 3.2.2 shows the 3D model of the modified vehicle with the modem/USBL developed by Newcastle University and an extra lateral thruster.

a)

MEDUSA$_D$ (Diver) Particulars	
Length	1035 mm
Height	875 mm
Tube diameter	150 mm
Weight in air	30 kg
Energy (LiPo)	830 Wh
Endurance	9 h at 1.5 knot
Propulsion System	5 thrusters

b)

Fig. 3.2.1 The MEDUSA$_D$ vehicles: a) isometric view, b) main particulars

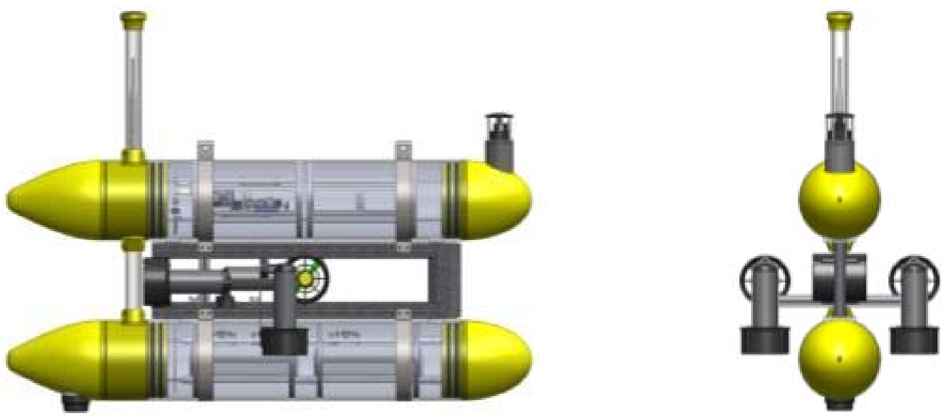

a) b)

Fig. 3.2.2 The MEDUSA$_D$ vehicles: a) side view, b) front view

2.2.3 e-URoPe AUV

The assembly of the vehicle is almost complete. The sequence reported in Fig. 3.2.2.1 shows the assembly phases: mounting of the frame and main electronics cylinder, installation of the buoyancy and thruster supports, thruster bodies, propellers, nozzles, illumination system.

Fig. 3.2.2.1. e-URoPe AUV assembly phases

The final assembly of the vehicle is shown in Fig. 3.2.2.2.

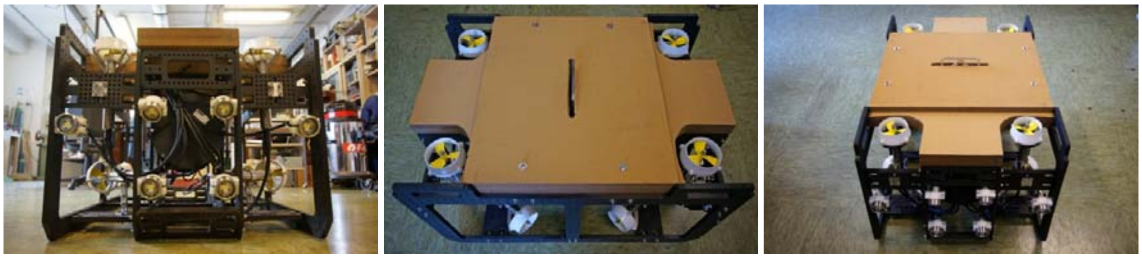

Fig. 3.2.2.2. e-URoPe AUV final assembly

The thruster force characteristics has been identified in order to be included in the dynamical modeling of the vehicle and it is reported in the plot of Fig. 3.2.2.3. The overall identification procedure will be carried out in a short time, after the completion of the vehicle assembly.

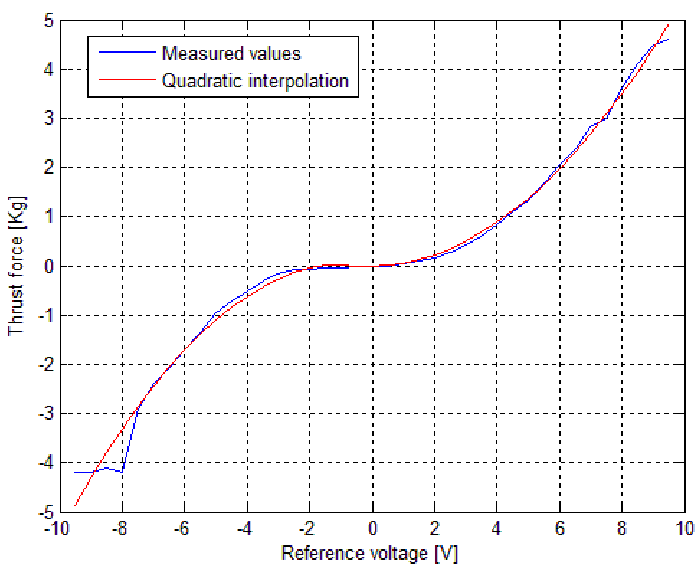

Fig. 3.2.2.3. e-URoPe AUV thruster force curve

3 Software integration

This section describes the different software modules developed to achieve the functionalities required for diver operation support

3.1 Diver compliant robotic task management

The aim of providing a compliant behavior of the overall robotic system, with respect to the operations undertaken by the diver, is made available through the development of an automatic selection system for the execution of the proper autonomous robotic tasks.

First of all, the basic CADDY functionalities has to be mapped into subsets of tasks that can be provided by the robotic platforms. In order to define the primitives-tasks matching, an additional high-level task set has to be defined as cross-interface between the primitives and robotic task sets.

A preliminary definition of the three sets is reported in Fig. 4.1.1, where:

- functional primitives represent the macro-actions that the robotic platform has to carry out in order to support the diver operation and that are strictly related to the current functional mode (slave, guide, observer);
- high-level logical tasks are the interface between the primitives and the operative task provided by robot. This logical task set is common in the overall architecture and will provide the required functionalities activating the proper low-level tasks that are currently made available by the employed robotic platform;
- low-level robotic tasks are the actual implemented autonomous functionalities on the target robot, e.g. speed regulators, heading and depth controller, etc. Depending on the low-level task availability, the CADDY compliant mission control system will properly select which high-level functionalities can be activated allowing, in turn, the enabling of the required primitives to fulfil the mission operations.

For the automatic selection, activation and inter-task conflict management, a Petri net based execution control system, inherited from the CNR-ISSIA robotic framework, is under current development. The system is configured by means of a set of configuration files that specify, on one side, the capabilities of the robot in terms of autonomous tasks and, on the other side, the set of high level functionalities that the CADDY system has to provide for the diver support. A real-time Petri net engine models the logical interconnections among the tasks and primitives and, depending on the specific actions commanded by the diver, automatically handle the activation/deactivation of the proper task sets.

As an example, Fig. 4.1.2 reports the case of activation of the "Follow me" primitive; such a primitive requires the system to turn on the following functionalities: "go_to_depth" to reach and maintain a desired depth (i.e. the same of the diver); "go_to_2D_point_fa" is the procedure to track a 2D point (the diver position) for fully-actuated (fa) platforms, that generates proper horizontal velocities for point tracking; "turn_towards" enabling the auto-heading capability to always look towards the diver.

In turn, each of the high-level task has to be linked with one or more low-level tasks in order to physically execute the required actions:

- "go_to_depth" requires the activation of a depth_controller;
- "go_to_2D_point_fa" requires the activation of surge and sway velocity regulators;
-"turn_towards" enables the auto-heading controller.

The logical links between the high- and low-level layers are set on the basis of the input/output variables: the output generated by a high-level task is the input for one or more low-level tasks, e.g. "go_to_2D_point_fa" generates the *u* and *v* speed reference signals that feed the low-level speed controllers.

If, as a second exemplificative case, an under-actuated platform is employed, it implies in turn that the "sway_speed" controller is not available (due to the under-actuation, e.g. of a rudder based vehicle). The unavailability of this latter low-level task reflects on the inhibition of the "go_to_2D_point_fa". Anyway to fulfil the "follow me" primitive requirements, the system can automatically switch to the "go_to_2D_point_ua" that can drive the robotic platform towards the desired point generating proper surge velocity and heading signals. The activation of the "go_to_2D_point_ua" task goes in conflict with the "turn_towards" one, given the generation of the ψ reference signals by both the tasks. Detecting this logical conflict, as depicted in Fig. 4.1.3, the system deactivates the execution of the "turn_towards" (that, by user definition, has a lower priority with respect to the "go_to_2D_point_ua" in relation to the "follow me" primitive).

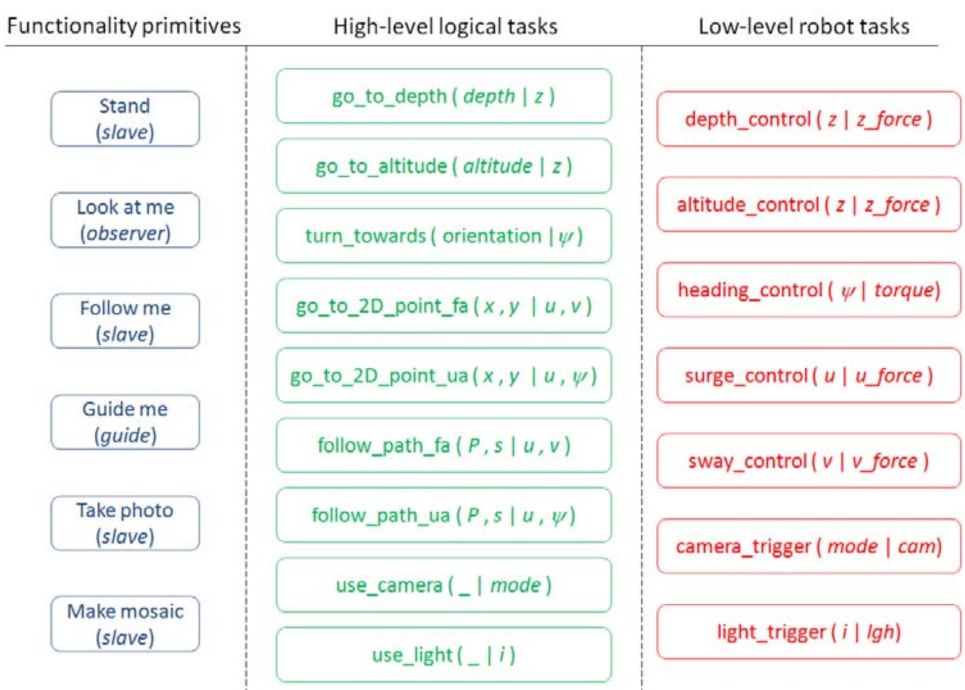

Fig. 4.1.1. Primitives and tasks definition

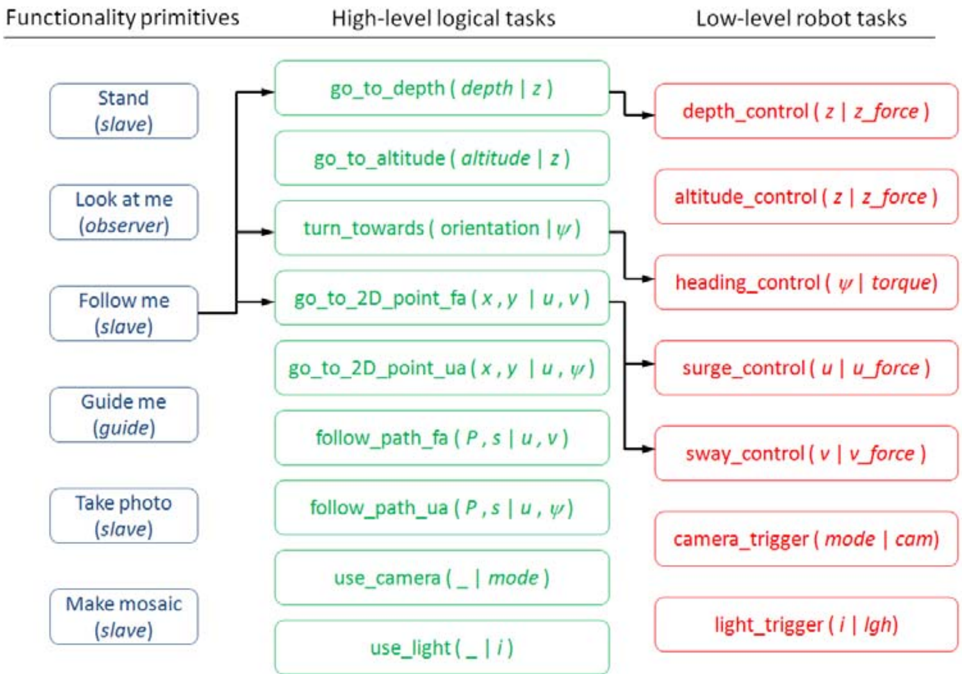

Fig. 4.1.2. Example of "follow me" primitive activation for fully-actuated robot

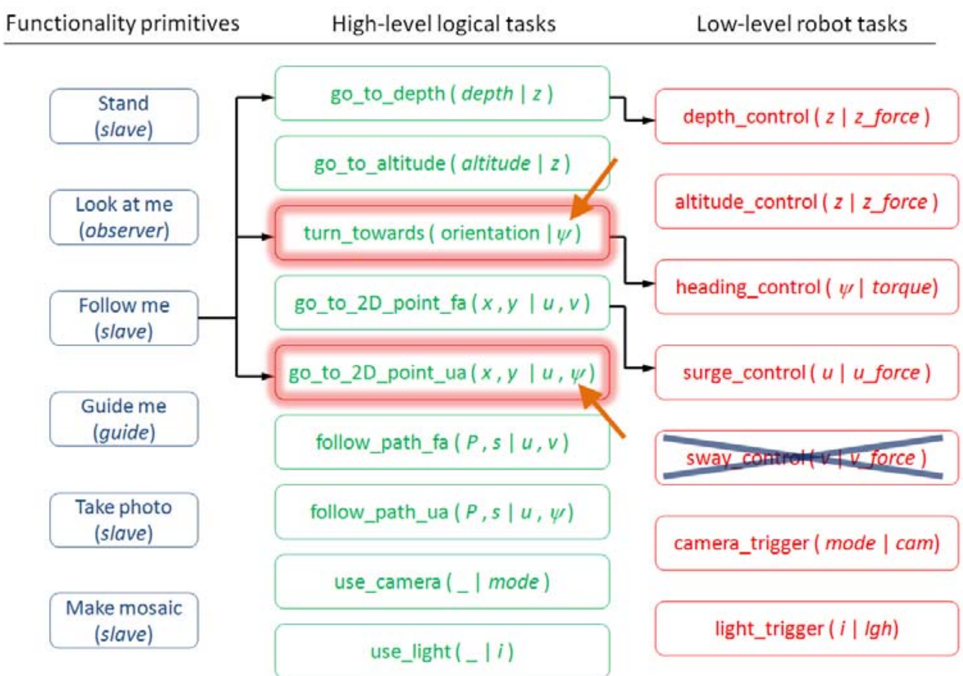

Fig. 4.1.3. Example of "follow me" primitive activation for under-actuated robot and inter-task conflict management

4 Simulation tests

This section reports the simulation results obtained by testing the different techniques and algorithms developed to fulfill and enhance the cooperation between the diver and the robotic system.

4.1 Cooperative guidance

An early simulation test has been carried out, in the scope of the cooperative guidance performance evaluation, through a HIL simulation environment common to the surface (Charlie ASV) and underwater (R2 AUV) robotic vehicles, both properly connected to the ROS environment through their relative wrappers, that allow the basic data exchange for the coordination task.
A common reference path is defined and sent to the vehicles; in a first totally virtual framework, the vehicles execute the path-following task (described in detail in Deliverable D4.1) and at the same time they exchange the virtual target curvilinear abscissa values in such a way to coordinate their speed and thus fulfilling the cooperative task. A 3D representation of the simulated experiment is depicted in Fig. 5.1.1, where the vehicles, after independently reaching the reference path, coordinate their speed in such a way to maintain a vertical configuration, with the ASV navigating on the surface and the dive buddy maintaining a constant depth.

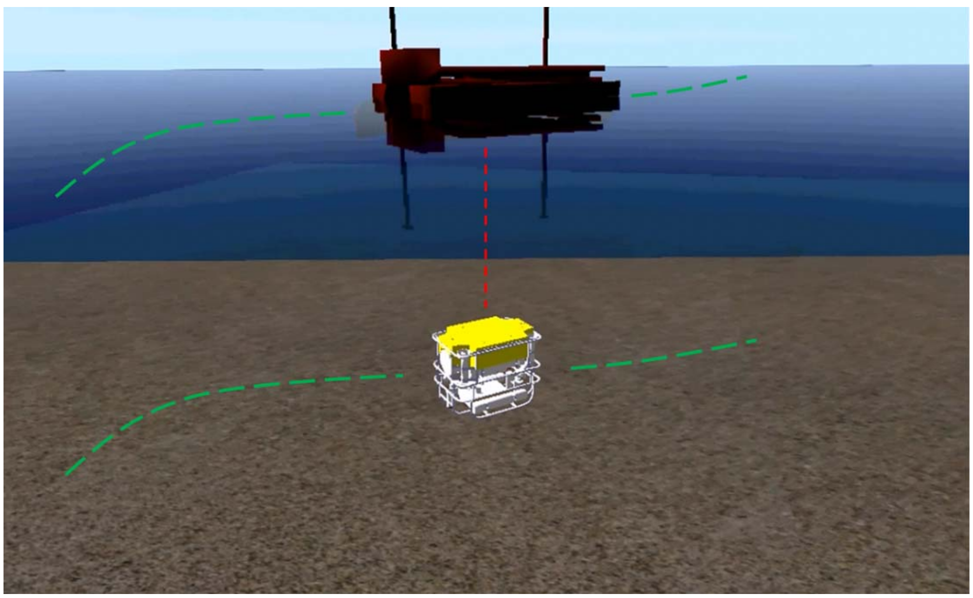

Fig. 5.1.1. Simulated cooperative guidance experiment

The horizontal motion of the vehicles during the experiment is reported in Fig. 5.1.2 where the different phases can be observed. Firstly, the vehicles perform the approach manoeuvre to the path; once on the path, they cooperatively regulate their surge speeds in order to reach and maintain the vertical formation. In the proposed simulation, at a certain time the dive buddy is required to force its speed to zero (triggered by any unpredicted event), thus losing the vertical formation with the ASV, that slows down to the minimum cruise speed trying to wait for the underwater vehicle to join back the formation. Once that the nominal operating condition is restored, the dive buddy accelerate to gain its formation position re-establishing the vertical configuration with the ASV.
In Fig. 5.1.3 the speed profiles of the two vehicles during the simulation are reported.

The simulation framework is made more complicated by the addition of the environmental uncertainties and disturbances as well as the communication delays introduced by the acoustic devices responsible for the data exchange. The simulation test is executed including the module responsible of the communication management; in the simulation framework, such a module generates disturbances and delays in virtual communication link, reproducing the acoustic medium behavior in water. Another simulation run is executed and the result is reported in Fig. 5.1.4, where the perturbed motions of the vehicles can be noticed; such motion behaviours don't impact the functionality of the cooperative guidance, anyway leading to the coordination task fulfilment.

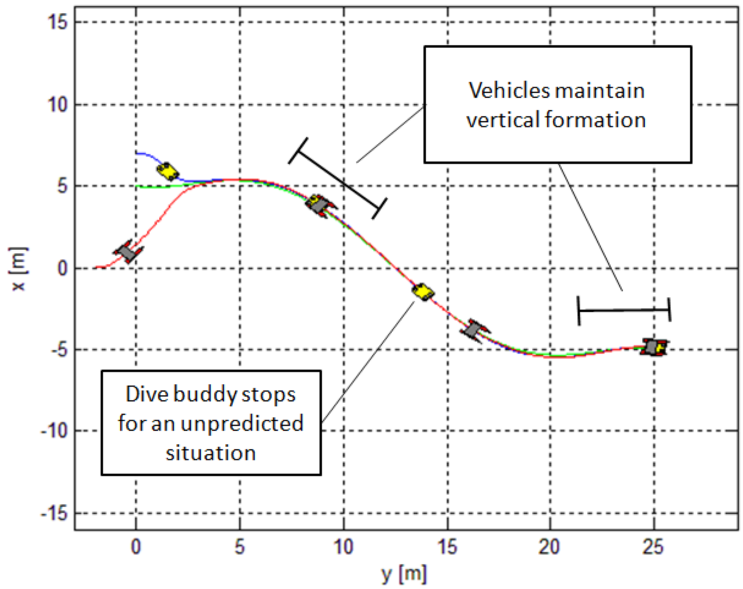

Fig. 5.5.3.2. Horizontal motion of the vehicles during the simulation

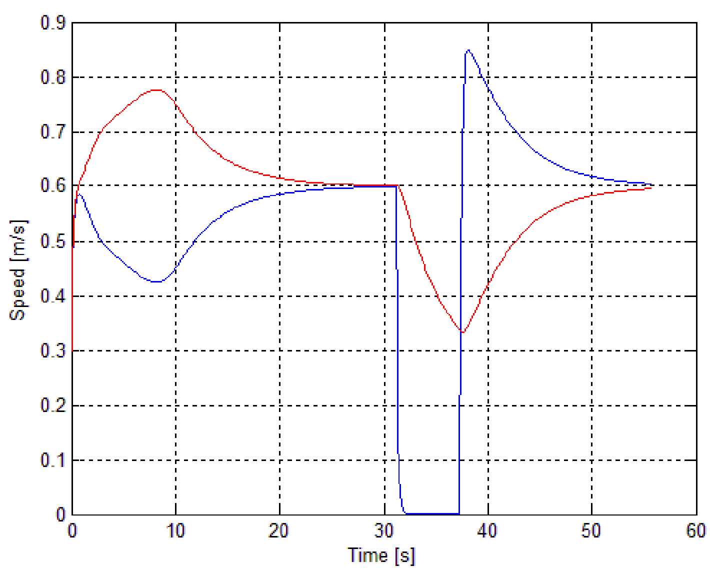

Fig. 5.5.3.3. Vehicle speed profiles during the simulation

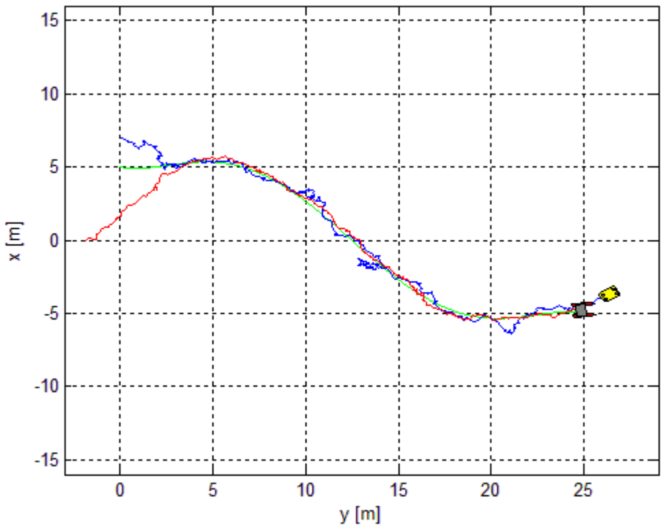

Fig. 5.5.3.4. Cooperation simulation corrupted by disturbances and communication delays

5 Experimental trials

5.1 Seatrac USBL data acquisition (Lisbon, Portugal, 2015)

As part of the effort towards integration of the Seatrac modems in the MEDUSA class of vehicles, a number of trials were designed to assess their performance in real conditions and validate the driver´s interface. The setup consisted of a fixed beacon, working in transponder mode, mounted on a tripod moored on the sea floor pointing upwards, and a USBL unit installed in one MEDUSA vehicle, pointing downwards. The underwater and surface components of the experiments are shown in the figure below.

Fig 6.1.1 Experiment setup with the fixed beacon on the tripod and the USBL mounted on the MEDUSA$_S$

A MEDUSA$_S$ vehicle performed a pre-programmed lawn mower mission at 0.3m/s while interrogating the fixed beacon at 0.5Hz. A 2D dispersion map and the error curves for bearing and range measurements were obtained. Most of the range errors are below 1m. The measurements of the bearing angles exhibit errors that must definitely be reduced. The data obtained are currently being examined in detail to take educated actions aimed at meeting the above objective.

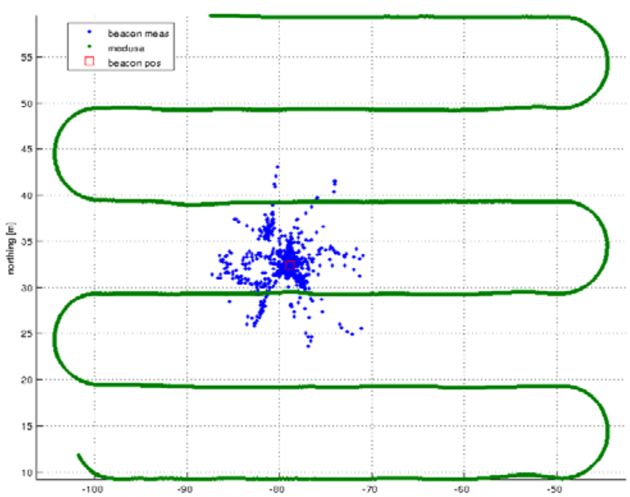

Fig 6.1.2 USBL fixes for a stationary beacon underwater

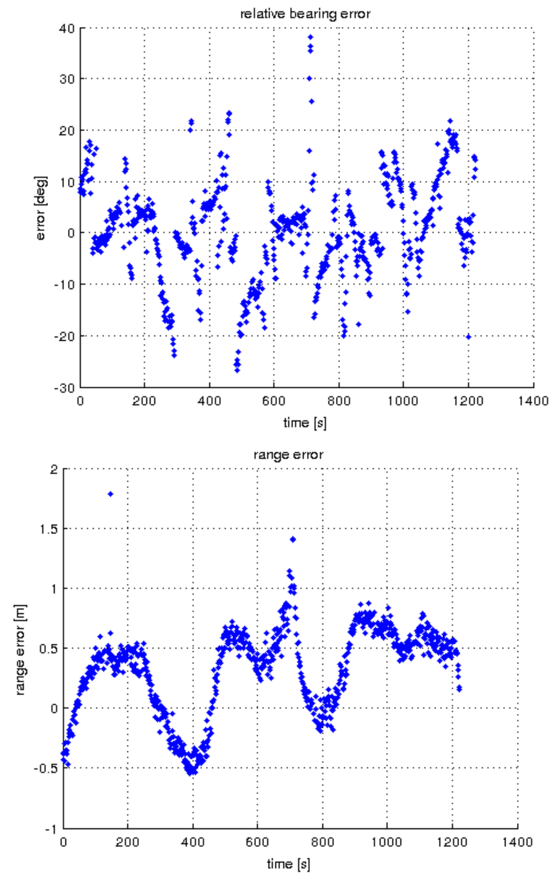

Fig 6.1.3 USBL Bearing and Range measurements against GPS positions

5.2 Surface Leader experiment, Lisbon, Portugal

In what follows, we summarize the results of practical experiments that illustrate the performance of the LTS (Leader Tracking System) in the first scenario: one ASV as leader and one AUV as follower. During the tests, the ASV was requested to perform a U-shaped path-following maneuver at the surface. In the set-up adopted, the virtual target (to be tracked by the AUV) is positioned at a point defined by desired along and across-path distances with respect to the path defined by the AUV (which is either a straight line or a segment of a circumference, or a combination thereof). The along and cross-path distances were set to -17 and +5 meters, respectively (intuitively speaking, this means that the AUV was requested to stay 17 meters behind along the path and 5 meters to the right). Throughout the maneuver, the AUV was commanded to remain at a fixed depth. The nominal speed of the leader vehicle (ASV) was set to 0.3 m/s.

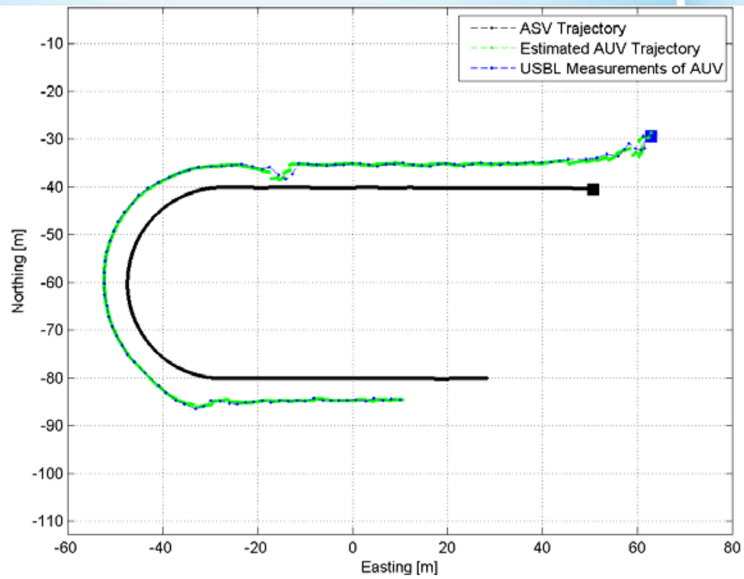

Fig. 6.2.1. Leader Tracking System with ASV as leader: ASV and AUV trajectories.

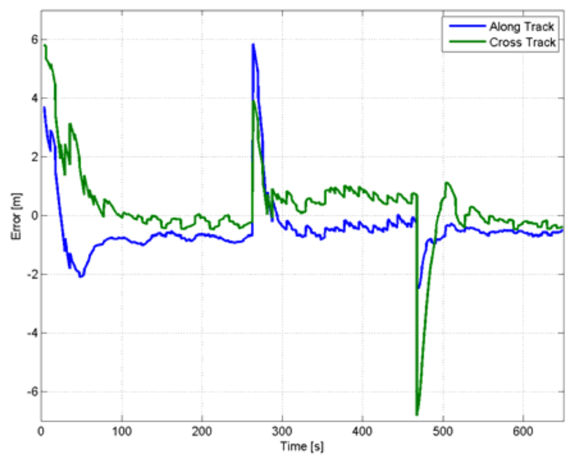

Fig. 6.2.2. Tracking error of the AUV

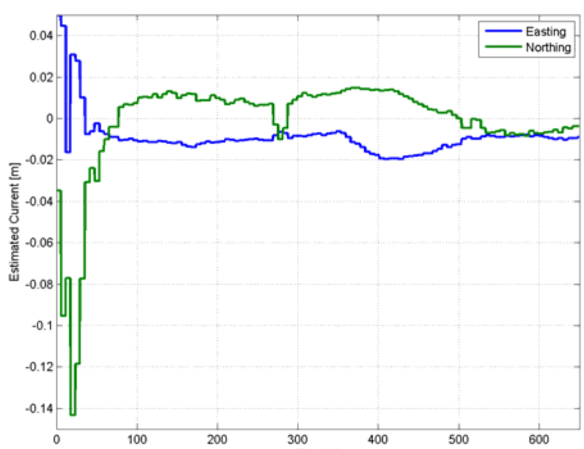

Fig. 6.2.3 Estimate of ocean current on-board the AUV

Fig. 6.2.1 shows the trajectories of both vehicles, and Figs. 6.2.2 and 6.2.3 show the position error (with respect to the virtual target that should be tracked) and the estimate of the ocean current. The performance of the Leader Tracking System illustrated by these figures is visibly good. The deterioration in performance that occurs when the ASV enters or leaves the circular part of the maneuver is simply due to the fact that the along- and cross track position specification for the virtual vehicle (to be tracked by the ASV) are done considering that the circular part of the path is extended backward as a circumference (upon detection that the ASV actually entered the circular path). This was done at the time when these tests were conducted to simplify the implementation of the Leader Tracking system. Meanwhile, this problem has been overcome by extending back the path taken by the AUV taking into consideration the actual path traversed, stored in memory. This is illustrated in the results shown in the next section, which no longer exhibit this problem.

5.3 Underwater Leader Experiment, Lisbon, Portugal

The second scenario is illustrated in Fig. 6.3.1 with results obtained with one AUV playing the role of leader, performing path-following on the same pre-defined U-shaped mission, and one ASV playing the role of follower. The ASV was configured to follow 5 meters behind along the path of the leader, and 5 m to the right. The nominal speed of the leader vehicle (AUV) was set to 0.3 m/s.

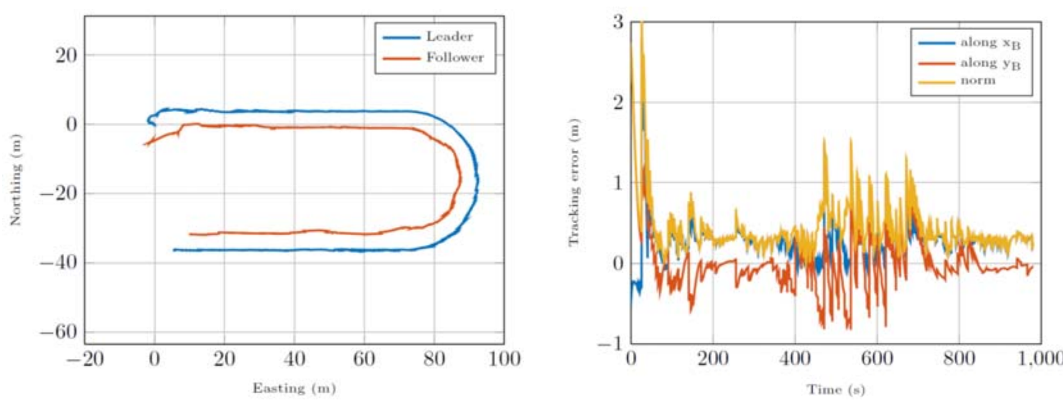

Fig. 6.3.1. Leader Tracking System with AUV as leader.
Left: Trajectories of AUV and ASV. Right Tracking error of the follower (ASV)

Again, the results are visibly good, with the tracking error of the follower (ASV) generally below 1 meter. The issue identified in the previous section when the leader vehicle enters or exits the turn has been effectively addressed and the performance no longer exhibits considerable deterioration in this situation, as happened in the previous scenario.

6 Conclusion

Initial experiments and performance analysis of the CADDY systems capabilities are reported in this deliverable.

The report describes the final hardware integration of the primary and backup vehicles, including the characterization of the different vehicles' features and performance evaluation during operations.

The deliverable also reports the description of the software modules developed to achieve the required functionalities, such as coordinated motion and diver motion compliance, in order to fulfill the CADDY requirements for the tasks of diver support.

Simulation results were performed to evaluate the reliability of the different software components needed to fulfill the different CADDY sub-goals, while experimental trials provided data for performance analysis of the system.